

BUCKLING BEHAVIORS OF ALUMINUM ALLOY DOUBLE LAYER TRUSS GRIDS USING BALL JOINT SYSTEM

by

YUJIRO HIYAMA¹, KOICHIRO ISHIKAWA², SHIRO KATO³

and

SHOJI OKUBO⁴

1 Sumitomo Light Metal Industries, LTD., Designing & Engineering Department, 5-11-3, Shimbashi,

Minato-ku, Tokyo 105, JAPAN, Phone;+81-3-3436-9847, Faccimli;+81-3-3436-9939,

E-mail: yujirou_hiyama@mail.sumitomo-lm.co.jp

2 Department of Architecture and Civil Engineering, Fukui University, 3-9-1, Bunkyo, Fukui-shi 910,

JAPAN, Phone;+81-776-27-8588, Faccimli;+81-776-27-8746,

E-mail: ishikawa@anc.anc-d.fukui-u.ac.jp

3 Department of Architecture and Civil Engineering , Toyohashi University of Technology,

Tempaku-cho, Toyohashi-shi 441, JAPAN, Phone;+81-532-44-6846, Faccimli;+81-532-44-6831,

E-mail; kato@sel17a.tut.ac.jp

4 Department of Architecture and Civil Engineering, Fukui University, 3-9-1, Bunkyo, Fukui-shi 910,

JAPAN, Phone;+81-776-27-8588, Faccimli;+81-776-27-8746,

E-mail: e960671@icpc00.icpc.fukui-u.ac.jp

Abstract

The usage of aluminum alloys as structural materials for buildings has been increasing owing to advantageous material properties, such as primarily a high strength to weight performance and corrosion resistance. With a strength equivalent to steel, the light weight characteristics of aluminum alloys are suitable for space structures that cover large spans. For the same reasons, aluminum alloys are effective as structural members in walls, because their use will often be beneficial through a reduction of dead load resting on the building foundations.

This study deals with the buckling behavior of aluminum alloy double layer truss grids composed of tubular members, ball joints and connecting bolts. In order to formulate a method for an appropriate analytical modeling for this kind of aluminum alloy structures, taking in consideration the factors such as aluminum material characteristics, member buckling , effects of the ball joints and the connecting bolts, tests of truss beams are carried out with varying slenderness ratio of the upper chords. From the buckling behaviors of the beams, it is confirmed that the rotational rigidity of the connections and the effective slenderness ratio of the members have a great effect on the pre and post-buckling behavior. Based on the test results, two modeling methods for the elastic-plastic analysis are proposed. And it is shown that both methods compared to the test results give a good corresponding result.

The buckling load and behavior of aluminum alloy double layer truss grids constructed by means of the ball joint system are investigated in this paper in accordance with the collapse modes by using the analytical method. The study gives design data useful enough to estimate the collapse modes and loads for this kind of aluminum alloy truss grid.

1. Introduction

Aluminum alloy is expected to be a suitable material for large span structures, because of a high strength relative to its specific gravity. On the other hand, aluminum alloy has material characteristics such as a high yield ratio and a decrease in strength after welding because of inherent properties of heat-treated alloys. Therefore, the structural design for aluminum alloys should be executed in consideration with the behavior after material yielding and with a proper evaluation of each ultimate strength, in case that the compression and the tensile forces reach approximately the same value like space truss.

This study deals with the system truss which uses the aluminum ball joint as the truss connection. For the double layered truss using the system truss as construction methods, the connection has been treated generally as a pin joint, and as a result, the evaluation of the buckling strength of truss member will be on the safe side. In other words, this type of connection is expected to provide some bending stiffness as explained Ref.(1), the actual buckling strength is expected to exceed the theoretical value for pin joints. However, such underestimation of the buckling strength relative to the tensile axial strength, is not always a safer design, because of the collapse modes being different from the original structural design.

Therefore the present study will introduce the buckling tests of the truss beam using aluminum ball joint for the connection and will investigate the effective slenderness ratio corresponding to the actual buckling strength of the truss members. And, from the results of the buckling tests, the post-buckling behavior of the truss member, relative to the member slenderness ratio, is discussed, in correspondence with past research in steel, Ref.(2),(3). Next, the buckling analyses are performed on the tested structural models making use of two modeling methods and the analytical method to simulate the structural tests is discussed. Furthermore, using the same two modeling methods, the buckling analyses are performed on a flat double layered truss, and the efficiency of such a non-linear analysis for the large scaled double layered trusses is discussed.

2. Loading test of the truss beam

2.1 Test method

Fig. 1 illustrates the figures and material standards of the aluminum alloy truss connections used in this study. The truss member called the "strut" is a tubular member. A conical fitting called the "end plug" is welded to the edge of the "strut". A bearing bolt is inserted in advance into a bolt hole at the center of the cross section of the end plug. The strut is connected with the solid ball, called the "hub", by screwing the bearing bolt. A pin is inserted into the bearing bolt in the cross sectional direction and enters the groove in the pipe-shaped collar. Thus, by rotating the collar, the bearing bolt can be screwed in, joining the strut to the hub.

All the applied struts, hubs, collars, and end plugs are extruded aluminum 6061 alloy, Al-Zn-Si heat-treated alloy. Bolts are high tension bolts made of Cr-Mo quenched and annealed steel.

Table 1 shows the constitutive members and their sectional properties. A total of four specimen

with different member slenderness ratios are prepared. Fig. 2 summarizes the experimental set-up of the buckling tests and measurements. The tightening torque of the collar is set at 29.4N·m. Two of the outer hubs are fixed, and the other two hubs are roller supported allowing for movement horizontally in longitudinal direction. In Fig. 2, the two upper chords of the truss beam are the observed buckling members, corresponding to S1 through S4 specimens in Table 1. The buckling tests were carried out in succession exchanging the upper chords for members with different member-slenderness ratio and investigate the respective buckling strengths and post-buckling behaviors. All the lower chords and the diagonal lattices are coded S5 member in Table 1. They are designed in such a way that yielding, in tension or in compression (buckling), does not occur, until the upper chords reach buckling loads.

The buckling stress σ_{cr} calculated from the following formula, as explained in Ref.(4), is shown in Table 1.

$$\sigma_{cr} = F \left\{ 1 - 0.5 \left(\frac{\lambda}{\Lambda} \right)^2 \right\} \quad : \text{ in the case of } \frac{\lambda}{\Lambda} \leq 1$$

$$\sigma_{cr} = \frac{F}{2 \left(\frac{\lambda}{\Lambda} \right)^2} \quad : \text{ in the case of } \frac{\lambda}{\Lambda} > 1 \quad (1)$$

Here λ is the slenderness ratio ($\lambda = \sqrt{L_k/i}$) where i is the radius of gyration and L_k is the unsupported length. In this study, the module length of the grid, 231 cm, is used for the value of L_k . The critical slenderness ratio Λ is calculated from

$$\Lambda = \sqrt{\frac{\pi^2 E}{0.5 \sigma_y}} \quad (2)$$

where a value of 0.5 is taken for the ratio of the elastic limit stress for an Euler's buckling load and, for the basic value F, the yield stress of 6061 aluminum alloy, 210Mpa is assumed.

A vertical load was applied to the center hub of the truss beam by using a 500kN hydraulic jack fixed to the reaction frame setting on the test bed. Two specimen were prepared, and the testing procedure for each specimen was programmed as follows: (1) Loads were applied until the buckling of the objective upper chords was reached. (2) After the buckling, loads were cyclically applied from two to four until the relation between load and displacement showed nearly flat. With regard to the displacement, the loading hub was measured vertically and unsupported hubs of the lower chords vertically and horizontally by dial gauges. The strains on the members were measured on four sides of the cross section of the members as denoted by the circular marks in Fig. 1. For upper chords of the observed buckling members, the strain gauges were fixed at both ends and in the center of the members, because of the formation of a plastic hinge in the case of buckling.

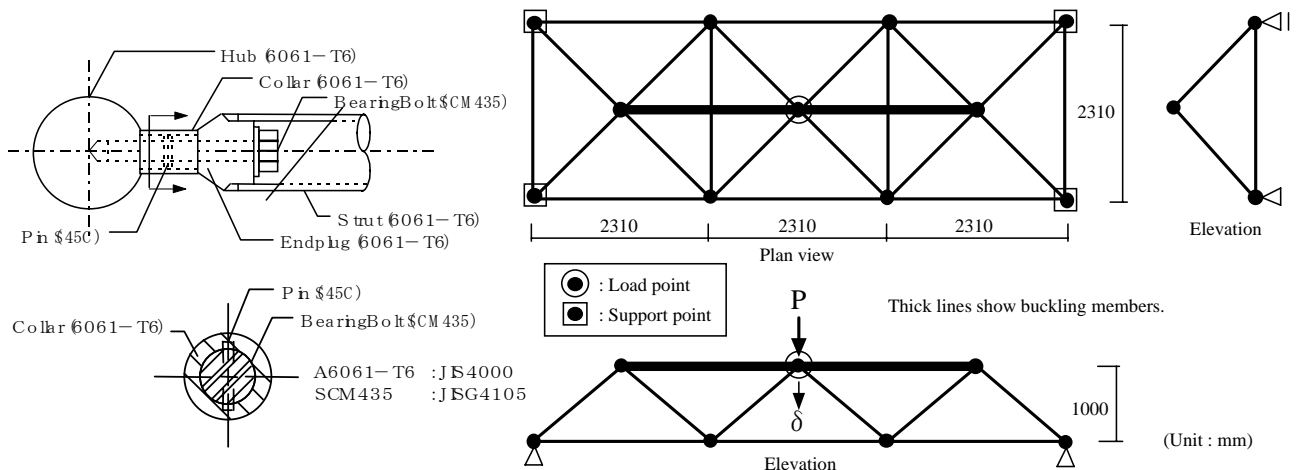
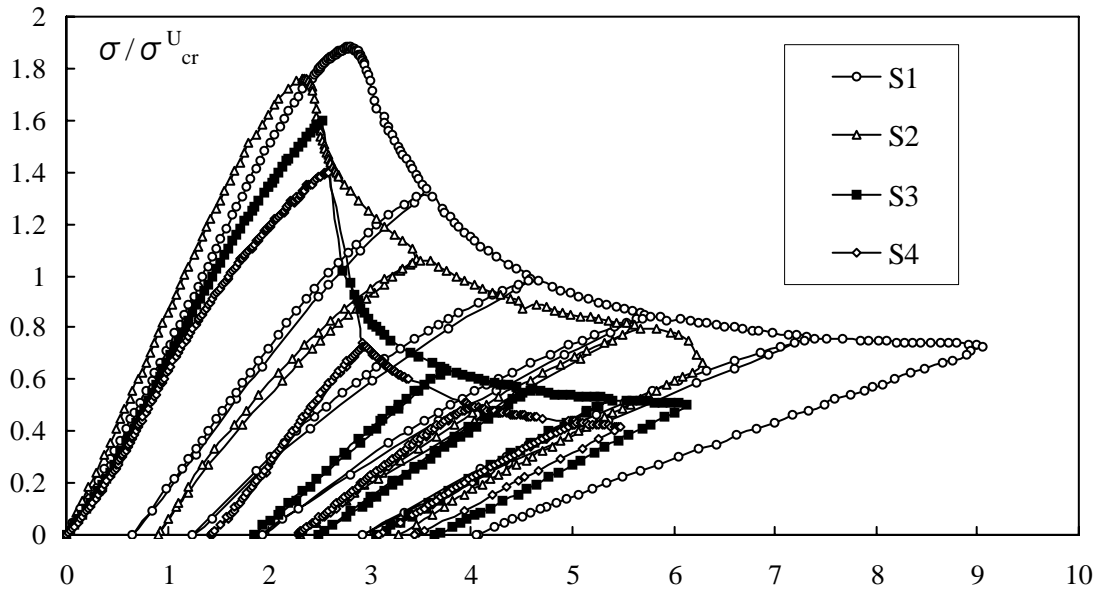


Table 1 Specimens used for buckling tests of the truss beams, theoretical buckling stress σ_{cr}^U and experimental buckling stress σ_{cr}^E

Specimens	Strut	Bolt	Collar	Hub	λ / Λ	σ_{cr}^U (GPa)	σ_{cr}^E (GPa)
S1	$\Phi 63.5 \times t6.35$	M20	$\Phi 40$	$\Phi 228$	1.40	0.054	0.099, 0.101
S2	$\Phi 63.5 \times t2.5$	M16	$\Phi 32$	$\Phi 228$	1.32	0.060	0.105, 0.105
S3	$\Phi 88.9 \times t7.6$	M27	$\Phi 54$	$\Phi 228$	0.99	0.105	0.169, 0.169
S4	$\Phi 100.0 \times t7.0$	M27	$\Phi 54$	$\Phi 228$	0.86	0.129	0.198, 0.185
S5	$\Phi 141.3 \times t12.7$	M39	$\Phi 78$	$\Phi 228$	0.62	0.146	-----

2.2. Test results and discussion

Fig. 1 Configurations and material standards of aluminum alloy truss Table 1 shows the buckling stress obtained from the test results. Fig. 2 Truss beam for buckling tests and analyses (For all the upper chords member type S1 to S4 is used and for all the lower chords member type S1 to S4 is used). Fig. 3 shows the relationships between the axial stress σ of the upper chord and the vertical displacement δ of the loading hub of the specimen S1 to S4. The axial stress σ is normalized by the theoretical buckling stress σ_{cr}^U in Table 1. Also the displacement δ is normalized by the elastic theoretical displacement of the buckling load for the truss beam which occurs at the theoretical buckling stress σ_{cr}^U . Fig. 4 shows the relationship between buckling stress σ_{cr}^E calculated from the test results and the member slenderness ratio λ , compared to the theoretical buckling stress σ_{cr}^U by the formula, as explained in Ref.(4). The theoretical buckling stress σ_{cr}^U is limited not to exceed the yield stress F_w of the welded parts. Therefore, the value 149MPa derived from $F_w / F = 0.71$ is used for the maximum



value of σ_{cr}^U .

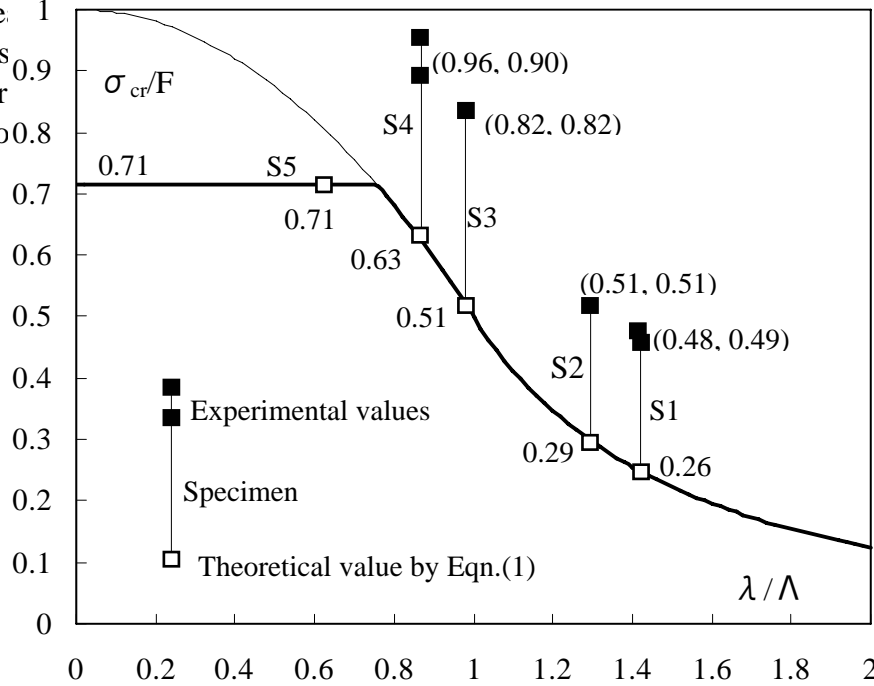
In Fig.3, all the specimens nearly experience linear behavior until the buckling load level, beyond which a sudden loss of the strength occur down to a low residual level. And it is noticed that the substantial sudden loss in the case of member type S3 and S4 with the slenderness ratios λ close to

the critical slenderness ratio Λ is observed. It is known well that the similar critical sudden loss occurs in this kind of steel members with around $\lambda / \Lambda = 1.0$.

With regard to the buckling stress in Fig. 4, the experimental values of S1 and S2, for which λ is larger than Λ , are 1.88 and 1.76 times the theoretical values. Similarly S3 and S4, for which λ is smaller than Λ , are 1.58 and 1.31 times the theoretical values, respectively. In other words, the experimental values of the buckling stress showed about twice the theoretical value in the region of Euler's buckling load.

When the relationship between the load and the displacement was deviated from linearity, the specimen began to swell in the welded parts at the ends of the members. Then, the maximum strength appeared.

After the specimen was loaded, after the welded section



During cyclic tests either in the

Fig. 4 Relationship between buckling stress σ_{cr}^E of the experimental results and the slenderness ratio λ , compared to the theoretical buckling stress σ_{cr}^U by Eqn.(1)

3. Numerical simulation

The elasto-plastic buckling analysis method considers the effects of geometric and material non-linearity of the members by using two kind of models including the beam-column and truss elements model. The purpose of the analysis is to compare analytical and experimental results concerning the elastic rigidities, buckling loads and post-buckling behavior of these space trusses.

Beam-column elements assuming rotational springs and rigid zones at both ends (analytical method A)

One analytical model assumes the members to be tubular aluminum beam-column elements with elasto-plastic springs at both ends and in the middle, as shown in Fig. 5. The elasto-plastic springs are assumed to behave elastically up to the yield point. Thereafter, the springs are assumed to flow plastically with the axial yield force N_Y and bending moments M_y and M_z (about the y and z axes,

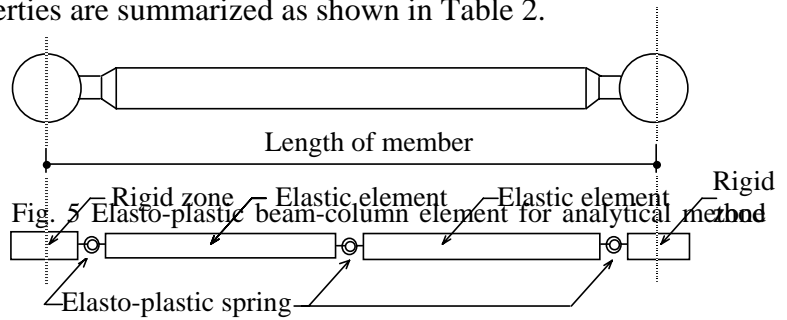
respectively) constrained to the yield surface defined by the following equation:

$$f = \left(\frac{N}{N_Y} \right)^2 + \sqrt{\left(\frac{M_y}{M_P} \right)^2 + \left(\frac{M_z}{M_P} \right)^2} = 1 \quad (3)$$

In eqn.(3), N is the axial force and M_P is the full plastic moment. The joints that are located at both ends of each member are modeled by elastic springs and are assumed not to yield. The stiffness matrix of the beam-column modeling is formulated by the slope deflection method with elastic member buckling. All the member properties are summarized as shown in Table 2.

Table 2 Axial yield force N_Y and full plastic moment M_P

Specimens	S1	S2	S3	S4
N_Y (kN)	234.6	98.6	399.5	420.9
M_P (kN·m)	4.29	1.92	10.37	12.49



Truss elements assuming pin-jointed member buckling under axial load (the analytical method B)

The other model assumes that the members constitute a pin-connected truss element. This model adopts the assumption that members buckle due to compression, and yield under tension. Fig. 6 shows the hysteresis curve used for a member slenderness ratio of $\lambda/\Lambda=1.0$. The maximum compressive stress σ_{cr} of the members is calculated by using Eqn.(1).

The hysteresis model for members adopts a plastic hinge concept including secondary effects due to lateral displacements and also includes plastic axial deformations of the hinge, together with elastic member shortening, see Ref. (6).

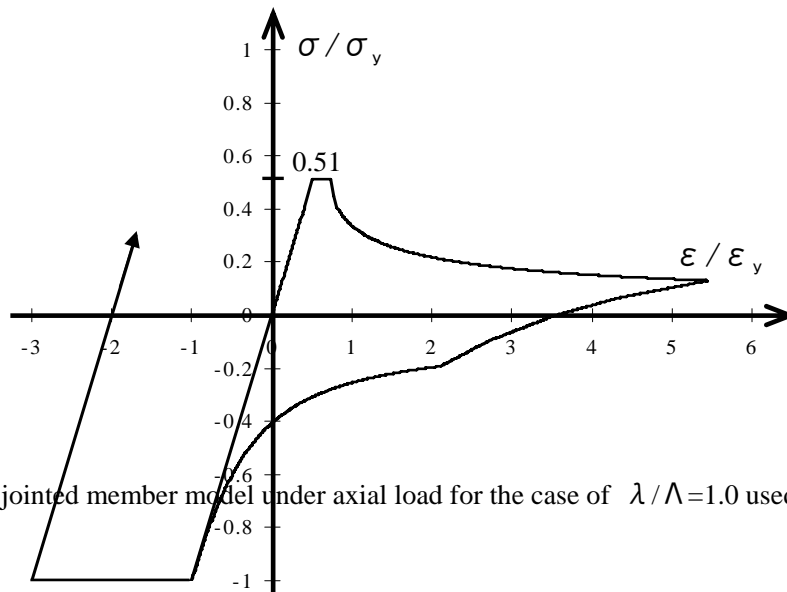


Fig. 6 Pin-jointed member model under axial load for the case of $\lambda/\Lambda=1.0$ used in method B

3-1. Comparison between analytical and experimental results for the truss beams

Elasto-plastic buckling analysis using the beam column element model (analytical method A)

The elasto-plastic analyses of the truss beams in Table 1 were carried out using the above mentioned beam column element method.

For the analyzed model of the truss beam, the bending stiffness of the joint may be taken to be half the value of the initial stiffness obtained in the experimental study dealing with this type of steel truss, see Ref. (6). The bending rigidity used for the analysis, in this paper is taken to be half the value of the initial stiffness, because this assumption gives buckling loads close to those found experimentally. The length of the rigid zone is taken to be equal to the radius of the hubs. The axial yield force N_Y and the full plastic moment M_P of the member type S1 to S4 are shown in Table 2. The mechanical properties of the constituent parts of the trusses are shown in Table 1. The axial rigidity of the joints is taken to be $0.4 \times 10^9 \text{N/m}$, which is an average value of compressive and tensile axial rigidities of the joints.

The relationships between the applied load P and the vertical displacement δ at the central node of the truss beam in Fig. 2 are obtained using this analytical method applied to the case of the trusses in which four different configurations(S1 to S4 in Table 1) were used for the upper chords. The results for two cases are shown in Fig.7 and 8. From the figures, it is seen that the analytical values show a good agreement with the experimental rigidities. Although not shown more, similar relationship were obtained by this analysis for the other cases.

The buckling loads calculated by analysis are much the same as the experimental buckling loads shown in Table 3. Accordingly, this analysis method can be estimated to provide a conservative estimation of the buckling loads of the trusses.

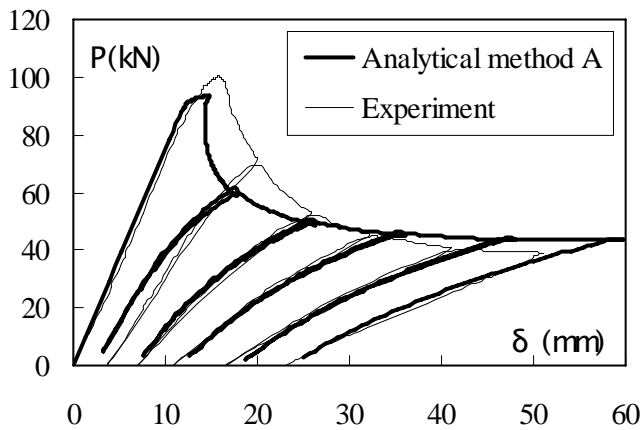


Fig. 7 Comparison of buckling curves between the analytical method A and the experiment in case of a truss beam with member type S1 for the upper chord

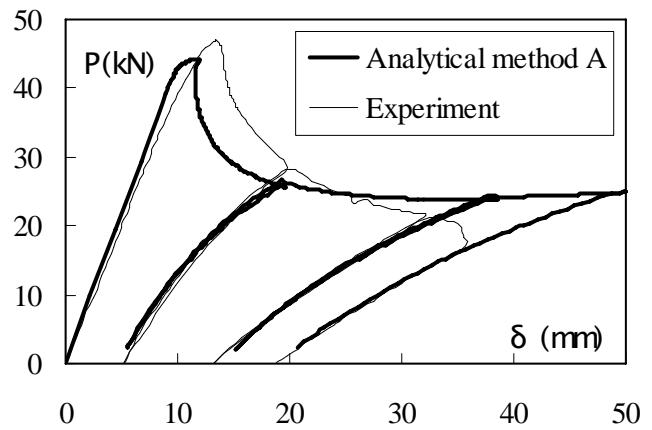


Fig. 8 Comparison of buckling curves between the analytical method A and the experiment in case of a truss beam with member type S2 for the upper chord

Table 3 Comparison of the maximum buckling loads of the truss beam with member type S1 to S4 for the upper chord obtained by the analytical method A and by the experiment

Member type for the upper chord	S1	S2	S3	S4
Maximum strength by experiment (kN)	100.0	47.0	284.2	320.5
Maximum strength by analysis (method A) (kN)	93.1	44.1	258.7	301.8
Analytical value (method A) / Experimental value	0.93	0.94	0.91	0.94

Elasto-plastic buckling analysis using the truss elements incorporating member buckling (the analytical method B)

An elasto-plastic buckling analysis of the truss beams was carried out using the pin-jointed truss elements mentioned above.

In this analysis, the cross-sectional areas of the members, which affect the rigidity of the truss beams, are taken to be those of the struts. The slenderness ratios of the members are assumed to be 70% of the values of the slenderness ratios derived from the lengths between the two end nodes of the member. Based on the experimental buckling load, the reduced slenderness ratio is evaluated.

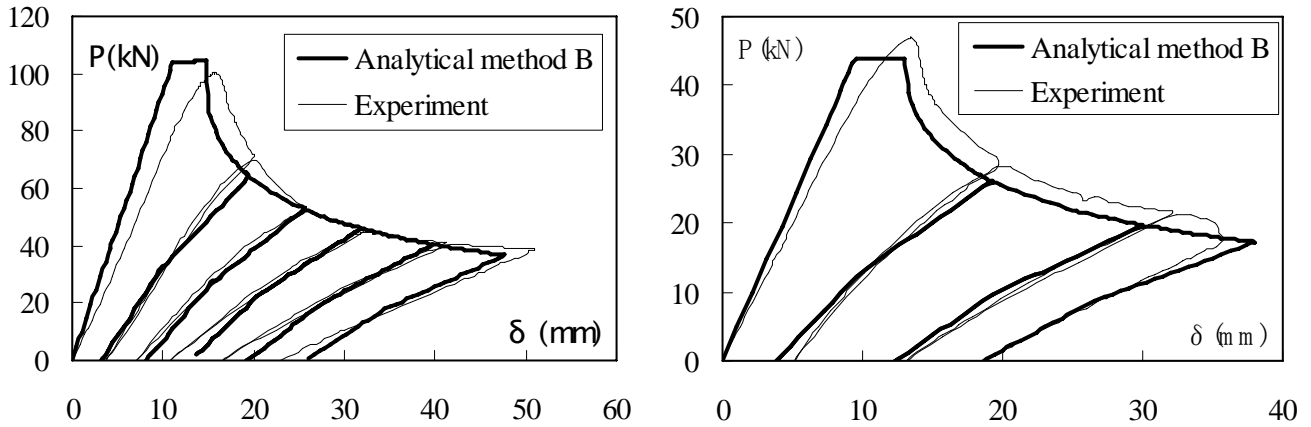


Fig. 9 and 10 compare the relationships between the vertical load P and the vertical displacement δ at the center of the truss beams in the two cases where the upper chord members are member type S1 and S2. It is seen that the analytical results such as the buckling loads and the buckling curves show good agreement with those of the experiments.

3-2. Comparison of both elasto-plastic buckling analysis methods for the truss grid

The elasto-plastic buckling analyses were carried out by using both analytical methods, A and B. The analyzed truss grid is shown in Fig. 11. For the upper chords of the truss grid member type S2 are used, for the lower chords and the diagonals member type S5 are used, as shown in Table 1. A vertical load P is applied at the central node of the upper chords. For boundary conditions, the four corners of the lower chords are restrained from displacements in the three directions.

Fig. 9 Comparison of the buckling curves between the analytical method B and the experiment in case of a truss beam with member type S1 for the upper chord

Fig. 10 Comparison of the buckling curves between the analytical method B and the experiment in case of a truss beam with member type S2 for the upper chord

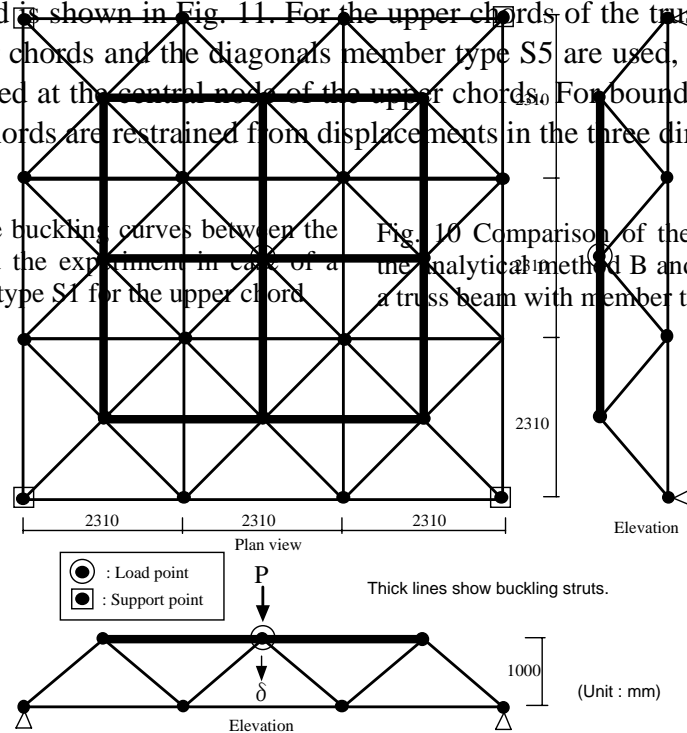


Fig.11 Analyzed truss grid (For all the upper chords member type S2 is used and for all the lower chords and diagonals member type S5 is used.)

Fig. 12 shows the relationships between the vertical load P and the vertical displacement δ in the central node, calculated by the analytical methods A and B. From the figure, the rigidities before buckling, the buckling loads, and the unloading paths after buckling show good agreement. But it is also seen that the flowing paths on the post-buckling process show some difference, probably, caused by the effects of the rigidities in the joints. For the collapse mechanism, all of the upper chords exhibit member buckling while other members, such as the lower chords and the diagonals, remain within the elastic region.

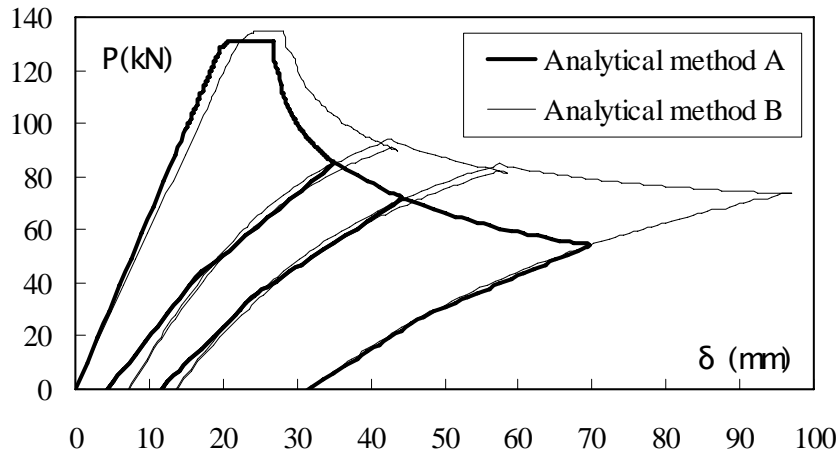


Fig.12 Comparison of buckling curves calculated using analytical method A and B in case of a truss grid

4. Conclusions

The conclusions of the present study can be stated as follows:

- 1) The experiment confirmed that the truss member using aluminum ball joints showed almost the same pre-and post-buckling behavior as expected for steel. Furthermore, it was confirmed that the reduction of the yield stress in the welds did not affect the buckling strength and post-buckling behavior.
- 2) The buckling stress obtained from the experiments was 1.8 times for members with $\lambda > \Lambda$ and 1.4 times for $\lambda < \Lambda$ greater than the theoretical values. It is considered that this behavior is probably a response to the effect of some existing bending stiffness in the connections. As a result, the effective member slenderness ratio, for the truss system, is predicted to correspond to 0.7 times the calculated ratio assuming the unsupported length L_k to be the distance between the grids.
- 3) Two analytical methods for the elasto-plastic buckling analysis of space truss structures (method A using the beam-column element and method B using the pin-ended truss element) were presented to investigate the possibility of predicting the buckling load and the load-displacement curves. The analytical method A and B dealing with the truss grid gave good agreement for the maximum buckling load and the unloading paths after buckling.
- 4) This simplifies that buckling behavior of space truss structures with a large number of members and joints may be simulated efficiently and rapidly on small computers using analytical method B.

References

- 1) Hiyama, Y., Takashima, H., Iijima, T., and Kato, S., "Experiments and Analyses of Aluminum Single Layered Reticular Domes", *IASS International Symposium*, pp.307-316, Nov., 1997,

Singapore

- 2) Saka, T. and Heki, K., "The Effects of Joints on the Strength of Space Trusses", Proceedings of the Third International Conference on Space Structures, Edited by H. Nooshin, pp. 417-422, September, 1984
- 3) EI – Sheikh, A., "Design of Space Truss Structures", Structural Engineering and Mechanics, Vol. 6, No. 2, pp.185-200, 1998
- 4) Society for Promotion of Aluminum Structures, "Aluminum Structural Design Manual", 1996
- 5) Ueki, T., Mukaiyama, Y., Shomura, M., and Kato, S., "Loading Test and Elasto-Plastic Buckling Analysis of a Single Layer Latticed Dome(in Japanese)," *Transactions of AIJ*, pp. 117-128, Mar., 1991
- 6) Igarashi, S., et al., "Hysteretic characteristics of steel Braced Frames (in Japanese)", *Transaction of AIJ*, No.196, pp.47-54, 1972